Importance of Metal-Ion Exchange for the Biological Activity of Coordination Complexes of the Biomimetic Ligand N4Py

Geersing, Arjan; Ségaud, Nathalie; van der Wijst, Monique G P; Rots, Marianne G; Roelfes, Gerard

Published in:
Inorganic Chemistry

DOI:
10.1021/acs.inorgchem.8b00714

Publication date:
2018

Inorganic Chemistry
Article
Cite This: Inorg. Chem. 2018, 57, 7748−7756
pubs.acs.org/IC

Importance of Metal-Ion Exchange for the Biological Activity of Coordination Complexes of the Biomimetic Ligand N4Py

Arjan Geersing,[†] Nathalie Ségaud,[†] Monique G. P. van der Wijst,[‡] Marianne G. Rots,*[,‡] and Gerard Roelfes*[,†]

[†]Stratingh Institute for Chemistry, University of Groningen, Nijenborgh 4, 9747 AG Groningen, The Netherlands
[‡]Department of Pathology and Medical Biology, University of Groningen, University Medical Center Groningen, Hanzeplein 1, 9713 GZ Groningen, The Netherlands

Supporting Information

ABSTRACT: Metal coordination complexes can display interesting biological activity, as illustrated by the bleomycins (BLMs), a family of natural antibiotics that when coordinated to a redox-active metal ion, show antitumor activity. Yet, which metal ion is required for the activity in cells is still subject to debate. In this study, we described how different metal ions affect the intracellular behavior and activity of the synthetic BLM-mimic *N*,*N*-bis(2-pyridylmethyl)-*N*-bis(2-pyridyl)methylamine (N4Py). Our study shows that a mixture of iron(II), copper(II), and zinc(II) complexes can be generated when N4Py is added to cell cultures but that the metal ion can also be exchanged by other metal ions present in cells. Moreover, the combination of chemical data, together with the performed biological experiments, shows that the active complex causing oxidative damage to cells is the Fe^{II}-N4Py complex and not per se the metal complex that was initially added to the cell culture medium. Finally, it is proposed that the high activity observed upon the addition of the free N4Py ligand is the result of a combination of scavenging of biologically relevant metals and oxidative damage caused by the iron(II) complex.

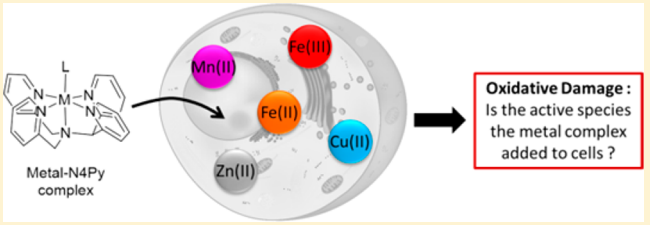

INTRODUCTION

Bleomycins (BLMs) are a family of natural antibiotics produced by *Streptomyces verticillus*[1] that are widely used as chemotherapeutic drugs to treat various types of cancer.[2] Coordination of a transition metal to its metal binding domain (i.e., Fe^{II} or Cu^{I}) results in the formation of metallobleomycins, which react with dioxygen under reductive conditions,[3] causing significant oxidative damage to cellular organelles and molecules.[4−9]

Extensive studies on BLMs in the past have indicated the importance of identifying the role of different metal species in the overall working of the drug in vitro. In cell-free systems, the activity of the metallobleomycins depends on the nature of the coordinated metal.[10−12] In these conditions, Fe^{II}-BLM shows the highest DNA cleavage activity, whereas the addition of excess Cu^{II}, Zn^{II}, or Co^{II} to BLM in the presence of Fe^{II} completely abolishes its activity.[12,13] In contrast, studies in cell cultures show comparable levels of antitumor activity between the different metallobleomycins (Zn^{II}, Cu^{II}, and $Fe^{II/III}$).[14,15] The comparable antitumor activity of the different metallobleomycins may hint toward a common metallobleomycin that is generated intracellularly by metal exchange.[14,16]

BLMs have inspired many ligands for the design of metal polypyridyl complexes, of which the ligand *N*,*N*-bis(2-pyridylmethyl)-*N*-bis(2-pyridyl)-methylamine (N4Py; Chart 1) has proven to be particularly successful.[17] Since its discovery, metal complexation of N4Py with Fe^{II},[17−19] Mn^{II},[20,21] Co^{II},[22] Ni^{II},[23] Cu^{II},[24] Zn^{II},[24,25] Ru^{II},[25−28] and Pt^{II}[29] has been reported.

Chart 1. Structure of the Ligand N4Py and the Metal Complexes in the Solid State as Used in This Study

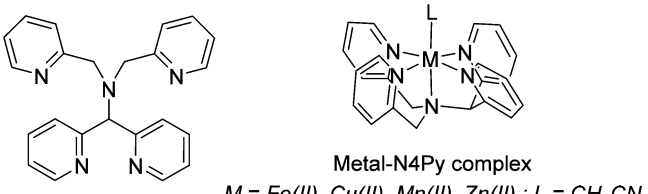

We have been particularly interested in the biological activity of N4Py. It has been shown in cell-free experiments that Fe^{II}-N4Py complexes exhibit significant DNA cleavage activity, which has been postulated to involve the formation of N4Py-Fe^{III}-OOH by reaction with reactive oxygen species (ROS) such as $O_2^{\bullet-}$ and H_2O_2.[30−35] Additionally, N4Py-Cu-OOH,[36] N4Py-Mn^{III}-O_2,[36,37] and N4Py-Mn^{IV}=O[38,39] species have been reported.

Received: March 21, 2018
Published: June 19, 2018

DOI: 10.1021/acs.inorgchem.8b00714
Inorg. Chem. 2018, 57, 7748−7756

Moreover, Fe^{II}-N4Py complexes exhibit high activity against various cancer cell lines, albeit via a different mechanism of action than BLM. Whereas BLM induces double-stranded DNA (dsDNA) breaks (DSBs) resulting in cell cycle arrest, N4Py was shown to induce apoptotic cell death.[40]

Interestingly, it was shown in this and other studies that also the free ligand exhibits biological activity. Jackson and Kodanko showed that N4Py can effectively bind and mobilize Fe^{II} from ferritin in aqueous solution.[41] Moreover, it was shown that N4Py can chelate Zn^{II} ions in cells, which was proposed to result in inhibition of the X-linked inhibitor of apoptosis protein (XIAP), resulting in cell death.[42] This study also suggested the ability of Fe^{II}-N4Py to generate ROS and induce apoptotic cell death. Combined, these studies raise questions about which metal complex is actually responsible for the biological activity in cells, which is increasingly recognized as an important aspect of the in vivo activity of coordination complexes.[43−50]

Here, we demonstrate that metal-ion exchange in the coordination of N4Py complexes is a very important aspect in the biological activity of N4Py coordination complexes. Particularly, we show that, irrespective of which metal ion was bound to N4Py initially, it is the iron(II) complex that is responsible for most of the observed activity. Our study demonstrates unequivocally that the intracellularly active complex does not necessarily correspond to the extracellularly added metal complex.

RESULTS AND DISCUSSION

Metal Binding Studies. Iron(II), iron(III), manganese(II), copper(II), and zinc(II) complexes of N4Py were synthesized following reported procedures (Supporting Information).[17,18,29,33,36,51] The complexes contain a molecule of acetonitrile on the sixth coordination site, with the exception of Fe^{III}-N4Py, which contains a methoxy ion as the axial ligand (L; Chart 1). The crystal structures from the different metal-N4Py complexes were compared (Figure S1 and Table S2), and some clear structural trends can be discerned. First, the average bond distances of the four equatorial M−N_{Py} bonds differ quite significantly, depending on the metal ion involved, with the average M−N_{Py} bond lengths for the manganese(II) complex being 0.28 Å longer than those for the iron(II) complex [2.251(8) Å over 1.971(8) Å, respectively]. The trend in the average M−N_{Py} bond lengths is manganese(II) > zinc(II) > copper(II) ≈ iron(III) > iron(II). Second, the position of the metal ion above the main plane of the four equatorial nitrogen atoms differs, with manganese(II) showing the most distorted structure, being 0.55 Å out-of-plane, while iron(II) shows the least distortion (0.21 Å).

The binding of N4Py to various metal ions in aqueous solution has been studied, although this was done in various conditions that are not necessarily representative for the conditions of biological experiments. Hence, spectroscopic characterizations of the various isolated complexes in solution were performed under conditions relevant to the cell culture studies (vide infra) as much as possible. The metal-N4Py complexes (0.5 mM) were dissolved in phosphate-buffered saline (PBS; 137 mM NaCl, 2.7 mM KCl, 10 mM Na_2HPO_4, 1.8 mM KH_2PO_4, pH 7.4, 37 °C), and their UV/vis absorption spectra and electrochemical properties were analyzed (Figure 1 and Table S3). All complexes showed pyridyl-centered ligand $\pi-\pi^*$ charge-transfer transition bands between 200 and 300 nm. The absorption spectrum for Mn^{II}-N4Py showed an additional weak shoulder around 320 nm (400 cm^{-1} M^{-1}). Cyclic voltammetry showed a $Mn^{III/II}$ irreversible oxidation at $E_{p,a}$ = 0.7 V vs Ag/AgCl.[20] The Fe^{II}-N4Py complex showed two resolved absorption bands at 377 nm (2000 cm^{-1} M^{-1}) and 460 nm (1450 cm^{-1} M^{-1}), assigned to metal-to-ligand charge-transfer (^{1}MLCT) transitions.[19] An irreversible $Fe^{III/II}$ redox process was observed at E_{pa} = 0.18 V vs Ag/AgCl. Correspondingly, the ferric complex showed a similar redox wave and had a near-UV absorption band at 370 nm (>2500 cm^{-1} M^{-1}).[33] For Cu^{II}-N4Py, a broad absorption band centered at 905 nm (170 cm^{-1} M^{-1}) and a higher energy shoulder around 730 nm (100 cm^{-1} M^{-1}) were observed. Cyclic voltammetry showed a reversible $Cu^{II/I}$ redox wave at E_{pa} = −0.42 V vs Ag/AgCl, which is in accordance with previous reports.[37] The zinc-coordinated complex is spectroscopically silent. In its voltammogram, the irreversible ligand redox wave at 1.02 V vs Ag/AgCl is absent,[52,53] which evidences binding of Zn^{II} to N4Py. This conclusion is supported by pronounced changes in the ^{1}H NMR chemical shifts of the ligand in comparison to N4Py alone (Supporting Information).

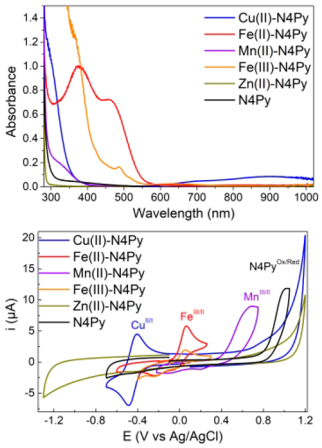

Figure 1. UV/vis absorption spectra (top) and cyclic voltammograms (bottom) of the metal-N4Py complexes (0.5 mM) in PBS (pH 7.4, 37 °C) under an argon atmosphere.

Next, it was investigated whether N4Py was able to bind these bioavailable metals in situ under cell-free conditions. The spectra and voltammograms of the solutions containing 1:1 N4Py/metal ratios are shown in Figure 2.

The addition of aliquots of iron(II) salt to a N4Py solution monitored by cyclic voltammetry showed the progressive disappearance of the ligand oxidation wave and simultaneous formation of the $Fe^{III/II}$ oxidation wave (Figure S2). Moreover, the addition of Fe^{II} ions caused the almost immediate formation of Fe^{II}-N4Py, as is evidenced by the typical ^{1}MLCT bands in the UV/vis spectrum (Figure S3). On the basis of the molar absorptivity determined for Fe^{II}-N4Py at 457 nm, a maximum conversion to the iron complex of 74% was observed (Table S4). Contrary to the case with iron(II) salt, the addition of iron(III) salt to N4Py did not result in the formation of a charge-transfer band in the absorbance spectrum, nor did it result in the disappearance of the ligand oxidation wave or the formation of an $Fe^{II/III}$ wave in the voltammograms. The addition of Mn^{II} ions to N4Py resulted in only the partial disappearance of the irreversible ligand oxidation peak and the appearance of a broad peak corresponding to the $Mn^{III/II}$ couple, suggesting that

DOI: 10.1021/acs.inorgchem.8b00714
Inorg. Chem. 2018, 57, 7748−7756

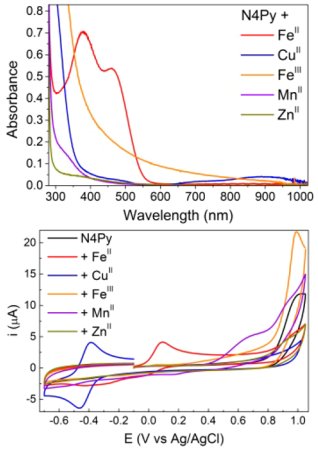

Figure 2. UV/vis absorption spectra (top) and cyclic voltammograms (bottom) after the stoichiometric addition of metal perchlorate salts to the N4Py ligand (0.5 mM) in PBS (pH 7.4, 37 °C) under an argon atmosphere.

coordination is not favored. The addition of Cu^{II} to N4Py resulted in the complete disappearance of the ligand oxidation wave and the appearance of the $Cu^{II/I}$ redox wave. However, formation of the broad absorption band around 900 nm (160 cm^{-1} M^{-1}) showed a maximum conversion of 50% (Figure S3 and Table S4). The addition of Zn^{II} to N4Py resulted in the complete disappearance of the ligand oxidation peak, suggesting that the Zn^{II}-N4Py complex is readily formed. On the basis of these results, it is evident that, under the indicated conditions, N4Py coordinates readily to Zn^{II}, Cu^{II}, and Fe^{II}, while the coordination of Mn^{II} is not favored and almost no coordination of Fe^{III} is observed.

The possibility for exchange of Fe^{II} ions from the N4Py complex with other biologically relevant metal ions was investigated by treating the Fe^{II}-N4Py complex (0.5 mM) with a variety of metal salts and monitoring the ^{1}MLCT band at 457 nm (Table 1 and Figure S4). During the time of the measurement, no decrease of this band was observed upon the addition of Mn^{II}, Fe^{III}, or Zn^{II} ions, suggesting that no metal exchange occurs. In contrast, in the presence of Cu^{II}, a decrease of the MLCT absorption band was observed, which suggests that 70% of Fe^{II}-N4Py was converted to Cu^{II}-N4Py, accompanied by the formation of the characteristic charge-transfer absorption band and reversible redox peak of the copper(II) complex (Figure S5).

Table 1. Metal-Ion Exchange in N4Py Coordination Complexes

metal ion added to Fe^{II}-N4Py[a]	conv to metal-N4Py (%)[b,c]	metal-N4Py[d]	conv to Fe^{II}-N4Py (%)[b,e]
Mn^{II}	0	Mn^{II}-N4Py	57
Fe^{III}	0	Fe^{III}-N4Py	100
Cu^{II}	70	Cu^{II}-N4Py	39
Zn^{II}	0	Zn^{II}-N4Py	44[f]

[a]Conversion of Fe^{II}-N4Py to the N4Py complexes of the indicated metal ions. [b]Conversions at t = 1500 s, at which time the absorption spectra had stabilized, suggesting that equilibrium is reached, unless noted otherwise. [c][N4Py] = 0.5 mM, [metal ion] = 0.5 mM, PBS buffer, pH 7.4. [d]Conversion of the indicated N4Py complexes to Fe^{II}-N4Py upon the addition of an iron(II) metal salt. [e][metal-N4Py] = 0.5 mM, [Fe^{II}] = 0.5 mM, PBS buffer, pH 7.4. [f]Because of slow exchange, the equilibrium had not yet been established at this time.

Subsequently, the inverse experiment was performed to study the ability of Fe^{II} to exchange with the different metal ions coordinated to N4Py, by following the formation of the ^{1}MLCT band at 457 nm in time (Figures S6 and S7 and Table 1).

The addition of Fe^{II} ions to a solution of Fe^{III}-N4Py resulted in the fast and complete conversion to the iron(II) complex, again suggesting the iron(II) complex is completely favored over its iron(III) analogue. Note, however, that the conversion is most likely the result of electron transfer, as opposed to the actual physical exchange of metal ions. In the case of Mn^{II}-N4Py, a majority of Mn^{II} is exchanged by Fe^{II} (57%), which indicates that binding of Mn^{II} to N4Py is very labile, and the addition of Fe^{II} ions leads to the rapid formation of a more stable product. Significant conversion of the copper(II) complex is observed (39%), albeit with much slower kinetics than that for manganese(II). Importantly, the conversion of Cu^{II}-N4Py to form Fe^{II}-N4Py is faster than the reverse process. This indicates that both Fe^{II} and Cu^{II} are quite inert in the N4Py environment, with a slight kinetic preference for Fe^{II}-N4Py. However, depending on the relative concentrations of the metal ions, a mixture of both complexes will thus most likely be present in cells. The zinc(II) complex is kinetically quite stable under the indicated conditions: even though almost half of the complex is converted to the iron(II) complex (44%), consistent with the reported K_d values for the zinc(II) and iron(II) complexes,[42,54] the kinetics are slow. In summary, Fe^{II} is thus capable of exchanging metal ions coordinated to N4Py, and the final degree of exchange is in the order Mn^{II} > Zn^{II} > Cu^{II}, a thermodynamic trend that is consistent with the Irving–Williams series.[55] Notably, the iron(II) complex itself does not fit in this trend; this is most likely because, at pH 7.4, there are multiple iron(II) species present, of which at least one is low spin and, hence, is kinetically more stable than the related high-spin complexes.[19]

DNA Cleavage Experiments. As a measure for the inherent catalytic activity, the DNA cleavage activities of the different metal-N4Py complexes were determined using supercoiled pUC18 plasmid DNA at 37 °C in the presence of dithiothreitol (DTT). Gel analysis after 30 min of incubation showed almost the complete disappearance of supercoiled DNA in the presence of Fe^{II}- and Fe^{III}-N4Py, while the other complexes did not show activity in DNA cleavage (Figure 3a). The average number of single-strand cuts per DNA molecule (n) was calculated from the amount of nicked and linear DNA formed (Figure 3b; for equations, see the Supporting Information). Clearly, the iron(II) and iron(III) complexes caused the largest number of single-strand cuts (5.5 ± 0.3 and 4.8 ± 0.3 cuts, respectively), with almost all supercoiled DNA consumed within 30 min. Evidently, in the cases of manganese(II), copper(II), and zinc(II), very little cleavage activity was observed (<0.3 cuts), indicating their almost negligible activity in cell-free systems.

Cell Studies. The biological activity of the metal-N4Py complexes was evaluated by MTS assay.[56,57] Two cancer cell lines (A2780 and SKOV3) and a noncancerous cell line (OSE-C2) were used in this study. Cells were treated for 24 h with different concentrations of N4Py and its metal complexes. The IC_{50} values for all cell lines were found to be in the range of 5–

DOI: 10.1021/acs.inorgchem.8b00714
Inorg. Chem. 2018, 57, 7748–7756

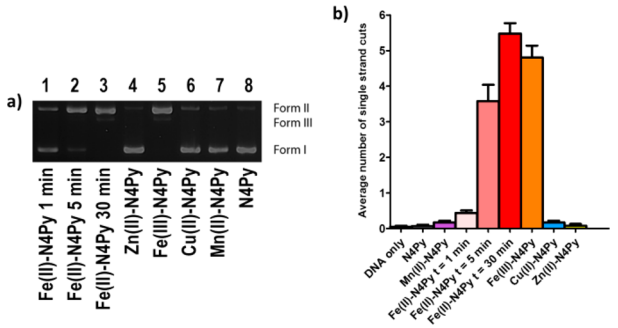

Figure 3. (a) Gel analysis of the cleavage of supercoiled DNA (form I) to give nicked DNA (form II) and linear DNA (form III) in Tris-HCl (pH 8.0) at 37 °C after 30 min (with the exception of lanes 1 and 2). Concentrations used: 1.0 μM complex, 0.1 μg μL^{-1} pUC18 plasmid DNA (300 μM in base pairs), and 1.0 mM DTT. (b) Average number of single-strand cuts per DNA molecule (n). Error bars represent the uncertainty limits of the data, based on a Monte Carlo simulation, taking into account a standard deviation σ of 0.03 of the individual DNA fractions. A correction factor of 1.31 was used to compensate for the reduced ethidium bromide uptake capacity of supercoiled DNA.[31]

10 μM for N4Py, Mn^{II}-N4Py, Fe^{II}-N4Py, and Fe^{III}-N4Py (Figure 4). Notably, an unusual sudden transition from high to

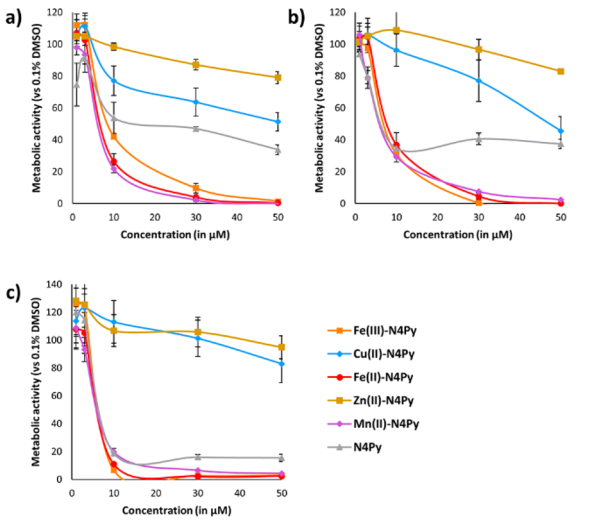

Figure 4. Metabolic activity (MTS assay) of (a) A2780, (b) SKOV3, and (c) OSE-C2 cell lines upon treatment with metal-N4Py complexes. Cells were treated for 24 h with 1, 3, 10, 30, and 50 μM N4Py and metal-N4Py complexes. Experiments were conducted three times. Within each treatment, each treatment was measured three times. Data are presented as the mean ± SEM.

almost no cell viability was observed for these compounds within this concentration range. This observation was in agreement with the cell viability, as assessed by light microscopy. The IC_{50} values for Cu^{II}-N4Py were around 50 μM, and treatment with Zn^{II}-N4Py resulted in hardly any decrease of the metabolic activity (IC_{50} > 50 μM).

The MTS assay can suffer from interfering processes.[58−64] Moreover, because the decrease in the metabolic activity can be explained by either cytotoxic or cytostatic processes, a propidium iodide (PI)/fluorescence-activated cell sorting (FACS) assay was performed. Cells will only stain PI positive once the cell membrane becomes permeable, i.e., when cells are late apoptotic or necrotic. The PI assay was performed by treating cells for 24 h with 10 μM of the metal complexes (Figure 5) because this was the lowest concentration where

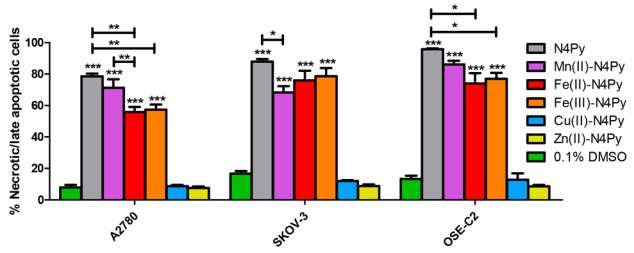

Figure 5. Cytotoxicity upon treatment with metal-N4Py complexes. The cell death was determined in A2780, SKOV3, and OSE-C2 cells treated for 24 h with 10 μM N4Py and its metal complexes [manganese(II), iron(II), iron(III), copper(II), and zinc(II)]. Cells were stained by PI, and the percentage of late apoptotic/necrotic cells was analyzed by FACS. Data are presented as the mean ± SEM from three independent experiments: ***, P < 0.001; **, P < 0.01; *, P < 0.05.

there were clear differences between the activities of different metal complexes (Figure 4). The Cu^{II}- and Zn^{II}-N4Py complexes showed the lowest cytotoxicity (5−10%), which correlates with their minor effect on the metabolic activity. Conversely, Mn^{II}-, Fe^{II}-, and Fe^{III}-N4Py showed significant amounts of cell death, ranging from 56% to 96%. Interestingly, N4Py, i.e., the free ligand, was found to be the most toxic compound in all three cell lines, with cell death levels varying from 79% (±1.8) in A2780 cells up to 96% (±0.5) in OSE-C2 cells. On the basis of the cell-free experiments, the cytotoxicity is expected to be induced by a metal-N4Py complex and not by the ligand alone. Therefore, this result suggests that the N4Py ligand is able to bind metals in the cellular environment. The combined data of Figures 4 and 5 clearly indicate that the decrease in the metabolic activity is mainly the result of a cytotoxic effect.

In view of the proposed oxidative mechanism of DNA cleavage in cell-free systems by Fe^{II}-N4Py and the reported oxo species of the Mn-, Fe-, and Cu-N4Py complexes (vide supra), it can be assumed that the cytotoxicity of the metal-N4Py complexes is a result of excessive ROS formation in the cells. In order to determine the intracellular formation of highly reactive oxygen species (hROS) upon treatment of the A2780 cells with the N4Py ligand and its metal complexes, the hROS probe 3′-(*p*-aminophenyl)fluorescein (APF) was selected (Figure 6).[65] Treatment of A2780 cells with N4Py gives a 2-fold (2.1 ± 0.1) increase in the fluorescence of APF versus 0.1% dimethyl sulfoxide (DMSO) control. This suggests that N4Py enters the cell and binds transition metal ions intracellularly to form complexes able to generate hROS. Zn^{II}-N4Py did not give rise to detectable ROS formation, which is in agreement with it being redox-inactive. Additionally, the exchange of Zn^{II} for Fe^{II} is slow (vide supra), suggesting that little of the Fe^{II}-N4Py complex is actually formed in the cells. In the presence of the other complexes, the amount of ROS detected increased between 1.6- and 2.3-fold with respect to DMSO.

Upon cotreatment with the antioxidant *N*-acetylcysteine (NAC), which protects cells from oxidants both directly, as a scavenger of free radicals, and indirectly, as a precursor for glutathione (GSH),[66−68] hROS production by cells treated

DOI: 10.1021/acs.inorgchem.8b00714
Inorg. Chem. 2018, 57, 7748−7756

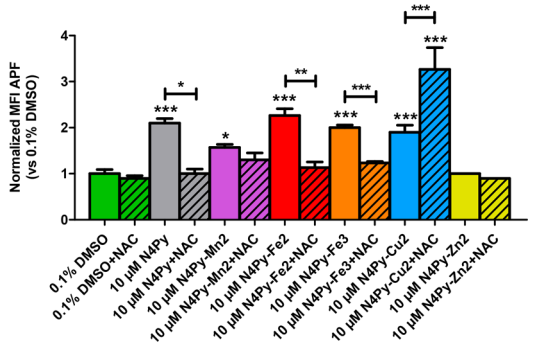

Figure 6. hROS formation upon treatment with metal-N4Py complexes. A2780 cells were treated for 24 h with the N4Py ligand, its metal complexes, or solvent control. The dashed columns represent the results obtained by cotreating with 5 μM of the antioxidant precursor NAC. hROS formation was detected by the ROS probe APF. Flow cytometric analysis of APF emission was used to obtain the mean fluorescent intensity (MFI) for each condition. The MFI was normalized to solvent control (green). Every experiment was carried out three times. Each bar shows the mean ± SEM: ***, $P < 0.001$; **, $P < 0.01$; *, $P < 0.05$.

with N4Py and all metal-N4Py complexes was completely abolished, except with Cu^{II}-N4Py (Figure 6). Remarkably, the amount of hROS detected was almost doubled from 1.9× to 3.3× versus 0.1% DMSO upon the cotreatment of Cu^{II}-N4Py with NAC. This is most likely caused by the reduction of Cu^{II} to Cu^{I} by NAC, which can then form a complex Cu^{I}-GSH that can react with molecular oxygen to produce ROS (vide infra).[69]

These results support an increase of the hROS levels in A2780 cells upon treatment with N4Py and its metal complexes. Thus, PI/FACS assay was repeated in the presence of two types of antioxidants: NAC or L-ascorbic acid 2-phosphate (AA2P)[70,71] (Figures 7 and S8). The level of cell death induced in the different cell lines (A2780, SKOV3, and OSE-C2) was comparable for each treatment. Interestingly, the presence of NAC or AA2P does not seem to impact the amount of cell death when cells are treated with N4Py or Mn^{II}-N4Py. On the contrary, cotreatment with NAC completely abolished the cell death induced by the Fe-N4Py complexes, with a clear effect of AA2P as well. Furthermore, the presence of NAC in the Cu^{II}-N4Py-treated cells resulted in a strong increase in cell death (up to 100% in A2780), indicating that the reduction of Cu^{II} to Cu^{I} by NAC not only induces hROS production by reaction with dioxygen but also, as a consequence, induces high levels of cell death. Treatment with AA2P had no effect on ROS formation by Cu^{II}-N4Py. Likewise, Zn^{II}-N4Py-treated cells showed no significant response to cotreatment with either NAC or AA2P.

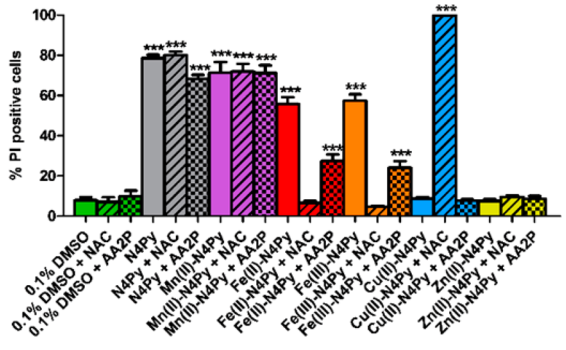

Figure 7. Effect of antioxidants (NAC and AA2P) on the metal-N4Py-complex-induced cytotoxicity. Cell death was determined in A2780 cells treated for 24 h with 10 μM N4Py and its metal complexes [manganese(II), iron(II), iron(III), copper(II), and zinc(II)]. Dashed and squared columns show cells cotreated with 5 μM NAC or 16 h pretreated and cotreated with 173 μM AA2P, respectively. Cells were stained by PI, and the percentage of late apoptotic/necrotic cells was analyzed by FACS. Data are presented as the mean ± SEM from three independent experiments: ***, $P < 0.001$; **, $P < 0.01$; *, $P < 0.05$.

Next, the ability of the different complexes in inducing oxidative DNA damage in vitro was studied. The extent of DSB formation was determined using flow cytometric detection of phosphorylated histone H2AX (γH2AX).[72] The histone protein H2AX forms a key component in DNA repair because it becomes rapidly phosphorylated at serine 139 and accumulates at emerging DSB sites.[73,74] After 24 h of treatment with 30 μM N4Py and its metal complexes, the percentage of γH2AX positive cells was determined in SKOV3 cells (Figure 8). Interestingly, significantly higher γH2AX levels compared

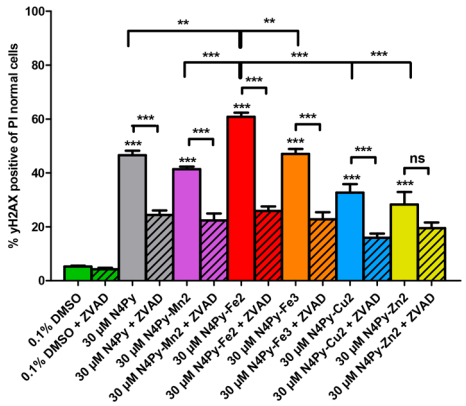

Figure 8. dsDNA damage (γH2AX) in nonapoptotic/early apoptotic cells induced by the metal-N4Py complexes. SKOV3 cells were treated for 24 h with 30 μM N4Py and its metal complexes. FACS analysis of γH2AX was used in combination with PI (marker for DNA content) to exclude late apoptotic cells (subG1 peak) from analysis. Cotreatment with 20 μM of the pan-caspase inhibitor ZVAD-FMK could reveal the contribution of apoptosis to the total DSB induction. The gate for γH2AX positive cells in solvent control was set at 5%. Each value represents the mean ± SEM from three independent experiments: ***, $P < 0.001$; **, $P < 0.01$; ns, not significant.

to the solvent controls were observed for all reagents ($P < 0.001$), which indicates that, at this concentration, nuclear DNA damage is induced by treatment with N4Py and all of the metal complexes. The iron(II) complex appears to produce slightly more dsDNA damage compared to the other reagents ($P < 0.001$ against Mn^{II}-, Cu^{II}-, and Zn^{II}-N4Py; $P < 0.01$ against N4Py and Fe^{III}-N4Py). The efficiency of metal-N4Py and N4Py for DSB is observed as follows: Fe^{II}-N4Py > N4Py ≈ Mn^{II}-N4Py ≈ Fe^{III}-N4Py > Cu^{II}-N4Py ≈ Zn^{II}-N4Py.

DSBs can be caused by various factors. Some reagents create DSBs directly, such as BLM and doxorubicin,[72,74] while others have an indirect effect, e.g., by triggering apoptosis.[75] To assess the contribution of apoptosis in the induction of DSBs by N4Py and the metal-N4Py complexes, SKOV3 cells were treated with the broad range caspase inhibitor carbobenzoxy-valyl-alanyl-aspartyl-[O-methyl]-fluoromethyl-ketone (ZVAD-

DOI: 10.1021/acs.inorgchem.8b00714
Inorg. Chem. 2018, 57, 7748−7756

FMK).[76] Upon the addition of ZVAD-FMK, a large reduction of 46−57% in the γH2AX levels was observed for all compounds except for Zn^{II}-N4Py, where a 20% reduction was obtained (Figure 8). This suggests that about half of the observed dsDNA damage is the result of apoptosis induced by N4Py or metal complexes. Nevertheless, even after inhibition of the caspase-dependent apoptosis pathway, the amount of observed dsDNA damage was still significant for all reagents ($P < 0.05$ for Cu^{II}-N4Py and $P < 0.001$ for N4Py and Mn^{II}-, Fe^{II}-, Fe^{III}-, and Zn^{II}-N4Py), suggesting that direct DNA damage is induced by N4Py or that also other cell death mechanisms may be involved.

Relationship between the Metal-Ion Coordination and Biological Activity. In this study, we described how different metal ions affect the intracellular properties of the synthetic BLM-mimic N4Py. Combined, these findings give rise to the following hypothesis (Scheme 1): we propose that

Scheme 1. Overview of the Coordination Chemistry of N4Py in Tumor Cells

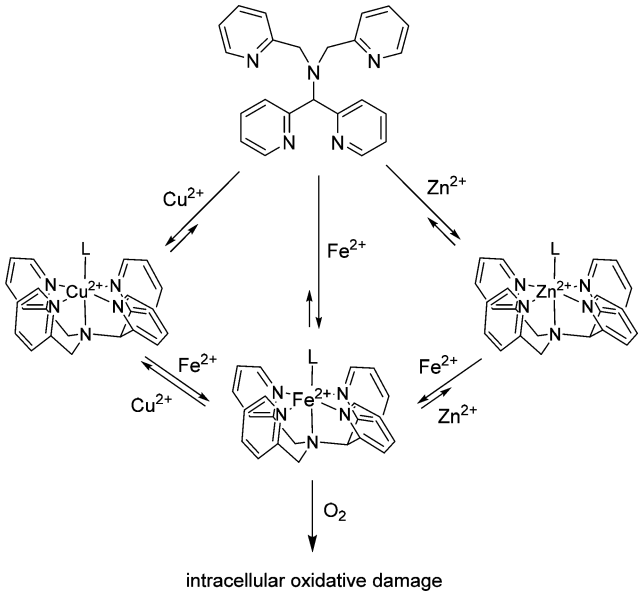

the main active complex that causes oxidative damage to the cell is the Fe^{II}-N4Py complex, irrespective of the initial metal ion coordinated. This is supported by the following arguments:

(i) The structural and binding studies show that, while most of the common bioavailable metal ions bind to N4Py, formation of the iron(II) complex is the most favorable and exchange of the bound metal ion for Fe^{II} occurs, albeit that it should be noted that the thermodynamically most stable complex is not necessarily catalytically active.

(ii) In cell-free experiments, Fe^{II}-N4Py is the only complex that showed oxidative DNA cleavage activity. In contrast, intracellularly, DSBs were generated with all metal complexes, albeit with different efficiencies: the addition of Fe^{II}-N4Py gave the highest number of DSBs, whereas Cu^{II}-N4Py and Zn^{II}-N4Py gave rise to the lowest number. It was shown that at least part of these DSBs are directly generated by the metal-N4Py complex itself, whereas the rest are generated indirectly, i.e., via the induction of apoptosis. This is in line with our previous in vitro observations for the Fe^{II}-N4Py complex.[40]

(iii) It is proposed that the observed oxidative damage, in part, can be ascribed to direct oxidation by the Fe-N4Py complex, which seems to be the only complex of N4Py that is capable of oxidizing cellular components, such as DNA. Even though formation of an N4Py-Cu−OOH species has been reported,[36] it was found to be a sluggish oxidant. Similarly, many Mn-oxo complexes show much less reactivity in oxidation reactions than their Fe-oxo counterparts.[77] Because coordination of Mn^{II} to N4Py does not appear to be favorable and Mn^{II} is readily exchanged for Fe^{II}, it is likely that mainly metal exchange, forming the Fe^{II}-N4Py complex, is responsible for the observed intracellular activity. In addition, Zn^{II} is not redox-active.[78]

(iv) Both iron(II) and iron(III) complexes are very active in the cleavage of supercoiled pUC18 plasmid DNA. The similarity in the cleavage activity is expected because the presence of a large excess of DTT will force the ferric complex into a ferrous complex. Similarly, the reducing conditions in the cell will convert the iron(III) complex into the iron(II) complex and, therefore, essentially give the same biologically active complex involving an oxidative mechanism of action.[79,80] The cytotoxicity of all metal-N4Py complexes in living cells can therefore principally be ascribed to the Fe^{II}-N4Py complex.

Some apparent contradictions in the presented data further support our hypothesis:

(i) The high kinetic stability of the Zn^{II}-N4Py complex is likely to account for its low cytotoxicity in the cell. Exchange with the more favored Fe^{II} ion is possible, albeit limited by the slow exchange rate. In line with this, no hROS formation was observed upon treatment with Zn^{II}-N4Py. The slight increase in DSBs may be accounted for by the slow exchange with Fe^{II} in the N4Py complex.

(ii) Cu^{II}-N4Py seems to be the most preferred complex under physiological conditions, as a significant, albeit minor, species. The lack of pUC18 plasmid DNA cleavage activity suggests the low oxidizing power of the copper(II) complex. Generally, the cell studies with Cu^{II}-N4Py resulted in little cytotoxicity to the cells at low concentrations, supporting that the copper(II) complex is the most prevalent complex even though the presence of iron(II) can result in formation of the Fe^{II}-N4Py complex. This suggests that the elevated concentrations of copper following the addition of the copper complex, rather than the physiological copper concentration, contribute to the favored formation of the copper complex.[81,82]

(iii) The high cytotoxicity and related high hROS levels detected for Cu^{II}-N4Py in the presence of NAC seem to be a direct result of Cu^{II} interaction and complex formation with GSH to form Cu^{I}-$(GSH)_2$, resulting in strongly elevated ROS levels.[69,83−85] This result is in agreement with the reported interaction of BLM with Cu^{II} in the presence of a reducing agent.[86−89]

Interestingly, the cellular damage induced by treatment of the free ligand N4Py is even higher than that obtained with the corresponding metal complexes. We propose that this can be ascribed by the combination of two effects:

(i) Intracellular chelation of the different metals contributes to the cytotoxicity observed for N4Py. From the binding competition experiments and the association/dissociation constants for the different metals as found in the literature, it can be deduced that the N4Py ligand may act as a Zn^{II},[42] Cu^{II}, and Fe^{II} chelator.[41] Therefore, by chelating, and, thus, scavenging metals, N4Py can influence many different cellular processes. For example, Zuo et al. have shown that Zn^{II} chelation by N4Py is associated with inhibition of the XIAP.[42] By chelating Zn^{II}, N4Py may induce apoptosis. In

DOI: 10.1021/acs.inorgchem.8b00714
Inorg. Chem. 2018, 57, 7748−7756

another case, N4Py was shown to successfully mobilize iron from ferritin (in 5 h, 5% of the total iron from ferritin is liberated),[41] the main intracellular iron storage protein.[90] This is in contrast to BLM, for which it was shown that it is unable to exchange metals with the iron storage proteins transferrin and ferritin.[87]

(ii) Additionally, the iron(II) complex of N4Py that is formed then is causing oxidative damage to the cells, as described above. Therefore, we propose that the increased cytotoxicity of the N4Py ligand compared to the Fe^{II}-N4Py complex can be ascribed to the additive effect of the intracellular chelation of metals, as well as oxidative damage. However, this study does not fully take into account the possible differences in the cellular influx of the different compounds, which can have an hitherto unknown influence on the final concentrations in the cells.

CONCLUSION

In this study, it was investigated how the coordination of different first-row transition-metal ions could influence the activity of the N4Py ligand in cultured cells. The results of our study indicate that a mixture of iron(II), copper(II), and zinc(II) complexes can be generated when N4Py is added to cell cultures. However, the combination of chemical data from analysis of the metal-N4Py complexes by UV/vis and cyclic voltammetry, together with the performed biological experiments, strongly suggests that the active complex that causes the oxidative damage to cells is the Fe^{II}-N4Py complex and not per se the metal complex that was initially added to the cell culture medium; that is, metal-ion exchange has to be considered in the analysis of the biological data.

ASSOCIATED CONTENT

Supporting Information

The Supporting Information is available free of charge on the ACS Publications website at DOI: 10.1021/acs.inorgchem.8b00714.

Details of the synthesis and characterization, physical measurements and biological experiments, and additional data of chemical and biological experiments (PDF)

Accession Codes

CCDC 1820683 contains the supplementary crystallographic data for this paper. These data can be obtained free of charge via www.ccdc.cam.ac.uk/data_request/cif, or by emailing data_request@ccdc.cam.ac.uk, or by contacting The Cambridge Crystallographic Data Centre, 12 Union Road, Cambridge CB2 1EZ, UK; fax: +44 1223 336033.

AUTHOR INFORMATION

Corresponding Authors

*E-mail: m.g.rots@umcg.nl.
*E-mail: j.g.roelfes@rug.nl.

ORCID

Nathalie Ségaud: 0000-0002-9221-1416
Gerard Roelfes: 0000-0002-0364-9564

Notes

The authors declare no competing financial interest.

ACKNOWLEDGMENTS

The authors thank Prof. E. Otten for determining the X-ray structure of Cu^{II}-N4Py. Financial support from The Netherlands Organisation for Scientific Research (Grant 728.011.101), the European Research Council (ERC Starting Grant 280010), the Ubbo Emmius Foundation of the University of Groningen, and The Netherlands Ministry of Education, Culture, and Science (Gravitation Program No. 024.001.035) is gratefully acknowledged. In addition, the authors acknowledge the H2020 COST Action CM1406 (www.EpiCHemBio.eu).

REFERENCES

(1) Umezawa, H.; Suhara, Y.; Takita, T.; Maeda, K. Purification of Bleomycins. *J. Antibiot.* **1966**, *19*, 210−215.
(2) Blum, R. H.; Carter, S. K.; Agre, K. A Clinical Review of Bleomycin–a New Antineoplastic Agent. *Cancer* **1973**, *31*, 903−914.
(3) Chen, J.; Stubbe, J. Bleomycins: Towards Better Therapeutics. *Nat. Rev. Cancer* **2005**, *5*, 102−112.
(4) Ekimoto, H.; Takahashi, K.; Matsuda, A.; Takita, T.; Umezawa, H. Lipid Peroxidation by Bleomycin-Iron Complexes in Vitro. *J. Antibiot.* **1985**, *38*, 1077−1082.
(5) Kikuchi, H.; Tetsuka, T. On the Mechanism of Lipoxygenase-like Action of Bleomycin-Iron Complexes. *J. Antibiot.* **1992**, *45*, 548−555.
(6) Rana, T. M.; Meares, C. F. Transfer of Oxygen from an Artificial Protease to Peptide Carbon during Proteolysis. *Proc. Natl. Acad. Sci. U. S. A.* **1991**, *88*, 10578−10582.
(7) Hecht, S. M. RNA Degradation by Bleomycin, a Naturally Occurring Bioconjugate. *Bioconjugate Chem.* **1994**, *5*, 513−526.
(8) Magliozzo, R. S.; Peisach, J.; Ciriolo, M. R. Transfer RNA Is Cleaved by Activated Bleomycin. *Mol. Pharmacol.* **1989**, *35*, 428−432.
(9) Stubbe, J.; Kozarich, J. W. Mechanisms of Bleomycin-Induced DNA Degradation. *Chem. Rev.* **1987**, *87*, 1107−1136.
(10) Hecht, S. M. Bleomycin: New Perspectives on the Mechanism of Action. *J. Nat. Prod.* **2000**, *63*, 158−168.
(11) Burger, R. M. Cleavage of Nucleic Acids by Bleomycin. *Chem. Rev.* **1998**, *98*, 1153−1170.
(12) Sausville, E. A.; Peisach, J.; Horwitz, S. B. Effect of Chelating Agents and Metal Ions on the Degradation of DNA by Bleomycin. *Biochemistry* **1978**, *17*, 2740−2746.
(13) Nagai, K.; Yamaki, H.; Suzuki, H.; Tanaka, N.; Umezawa, H. The Combined Effects of Bleomycin and Sulfhydryl Compounds on the Thermal Denaturation of DNA. *Biochim. Biophys. Acta, Nucleic Acids Protein Synth.* **1969**, *179*, 165−171.
(14) Rao, E. A.; Saryan, L. A.; Antholine, W. E.; Petering, D. H. Cytotoxic and Antitumor Properties of Bleomycin and Several of Its Metal Complexes. *J. Med. Chem.* **1980**, *23*, 1310−1318.
(15) Byrnes, R. W.; Templin, J.; Sem, D.; Lyman, S.; Petering, D. H. Intracellular DNA Strand Scission and Growth Inhibition of Ehrlich Ascites Tumor Cells by Bleomycins. *Cancer Res.* **1990**, *50*, 5275−5286.
(16) Lyman, S.; Ujjani, B.; Renner, K.; Antholine, W.; Petering, D. H.; Whetstone, J. W.; Knight, J. M. Properties of the Initial Reaction of Bleomycin and Several of Its Metal Complexes with Ehrlich Cells. *Cancer Res.* **1986**, *46*, 4472−4478.
(17) Lubben, M.; Meetsma, A.; Wilkinson, E. C.; Feringa, B.; Que, L. Nonheme Iron Centers in Oxygen Activation: Characterization of an Iron(III) Hydroperoxide Intermediate. *Angew. Chem., Int. Ed. Engl.* **1995**, *34*, 1512−1514.
(18) Roelfes, G.; Lubben, M.; Leppard, S. W.; Schudde, E. P.; Hermant, R. M.; Hage, R.; Wilkinson, E. C.; Que, L., Jr.; Feringa, B. L. Functional Models for Iron-Bleomycin. *J. Mol. Catal. A: Chem.* **1997**, *117*, 223−227.
(19) Draksharapu, A.; Li, Q.; Logtenberg, H.; van den Berg, T.; Meetsma, A.; Killeen, J. S.; Feringa, B. L.; Hage, R.; Roelfes, G.; Browne, W. R. Ligand Exchange and Spin State Equilibria of

DOI: 10.1021/acs.inorgchem.8b00714
Inorg. Chem. 2018, 57, 7748−7756

FeII(N4Py) and Related Complexes in Aqueous Media. *Inorg. Chem.* **2012**, *51*, 900−913.
(20) Young, K. J.; Takase, M. K.; Brudvig, G. W. An Anionic N-Donor Ligand Promotes Manganese-Catalyzed Water Oxidation. *Inorg. Chem.* **2013**, *52*, 7615−7622.
(21) Geiger, R. A.; Leto, D. F.; Chattopadhyay, S.; Dorlet, P.; Anxolabehere-Mallart, E.; Jackson, T. A. Geometric and Electronic Structures of Peroxomanganese(III) Complexes Supported by Pentadentate Amino-Pyridine and -Imidazole Ligands. *Inorg. Chem.* **2011**, *50*, 10190−10203.
(22) Xie, J.; Zhou, Q.; Li, C.; Wang, W.; Hou, Y.; Zhang, B.; Wang, X. An Unexpected Role of the Monodentate Ligand in Photocatalytic Hydrogen Production of the Pentadentate Ligand-Based Cobalt Complexes. *Chem. Commun.* **2014**, *50*, 6520−6522.
(23) Zhang, P.; Wang, M.; Yang, Y.; Zheng, D.; Han, K.; Sun, L. Highly Efficient Molecular Nickel Catalysts for Electrochemical Hydrogen Production from Neutral Water. *Chem. Commun.* **2014**, *50*, 14153−14156.
(24) Lo, W. K. C.; McAdam, C. J.; Blackman, A. G.; Crowley, J. D.; McMorran, D. A. The Pentadentate Ligands 2PyN2Q and N4Py, and Their Cu(II) and Zn(II) Complexes: A Synthetic, Spectroscopic and Crystallographic Structural Study. *Inorg. Chim. Acta* **2015**, *426*, 183−194.
(25) Kojima, T.; Weber, D. M.; Choma, C. T. { N -[Bis(2-Pyridyl)Methyl]- N, N -Bis(2-Pyridylmethyl)Amine-κ 5 N }-chlororuthenium(II) Perchlorate Methanol Solvate. *Acta Crystallogr., Sect. E: Struct. Rep. Online* **2005**, *61*, m226−m228.
(26) Ohzu, S.; Ishizuka, T.; Hirai, Y.; Fukuzumi, S.; Kojima, T. Photocatalytic Oxidation of Organic Compounds in Water by Using Ruthenium(II)-Pyridylamine Complexes as Catalysts with High Efficiency and Selectivity. *Chem. - Eur. J.* **2013**, *19*, 1563−1567.
(27) Ohzu, S.; Ishizuka, T.; Hirai, Y.; Jiang, H.; Sakaguchi, M.; Ogura, T.; Fukuzumi, S.; Kojima, T. Mechanistic Insight into Catalytic Oxidations of Organic Compounds by Ruthenium(Iv)-Oxo Complexes with Pyridylamine Ligands. *Chem. Sci.* **2012**, *3*, 3421−3431.
(28) Makino, M.; Ishizuka, T.; Ohzu, S.; Hua, J.; Kotani, H.; Kojima, T. Synthesis and Characterization of an Azido-Bridged Dinuclear Ruthenium(II) Polypyridylamine Complex Forming a Mixed-Valence State. *Inorg. Chem.* **2013**, *52*, 5507−5514.
(29) Lo, W. K.; Huff, G. S.; Preston, D.; McMorran, D. A.; Giles, G. I.; Gordon, K. C.; Crowley, J. D. A Dinuclear Platinum(II) N4Py Complex: An Unexpected Coordination Mode For N4Py. *Inorg. Chem.* **2015**, *54*, 6671−6673.
(30) Roelfes, G.; Branum, M. E.; Wang, L.; Que, L.; Feringa, B. L. Efficient DNA Cleavage with an Iron Complex without Added Reductant. *J. Am. Chem. Soc.* **2000**, *122*, 11517−11518.
(31) van den Berg, T. A.; Feringa, B. L.; Roelfes, G. Double Strand DNA Cleavage with a Binuclear Iron Complex. *Chem. Commun.* **2007**, 180−182.
(32) Roelfes, G.; Lubben, M.; Hage, R.; Que, L., Jr.; Feringa, B. L. Catalytic Oxidation with a Non-Heme Iron Complex That Generates a Low-Spin Fe(III)OOH Intermediate. *Chem. - Eur. J.* **2000**, *6*, 2152−2159.
(33) Roelfes, G.; Lubben, M.; Chen, K.; Ho, R. Y. N.; Meetsma, A.; Genseberger, S.; Hermant, R. M.; Hage, R.; Mandal, S. K.; Young, V. G.; Zang, Y.; Kooijman, H.; Spek, A. L.; Que, L.; Feringa, B. L. Iron Chemistry of a Pentadentate Ligand That Generates a Metastable Fe(III)-OOH Intermediate. *Inorg. Chem.* **1999**, *38*, 1929−1936.
(34) Roelfes, G.; Vrajmasu, V.; Chen, K.; Ho, R. Y. N.; Rohde, J.-U.; Zondervan, C.; La Crois, R. M.; Schudde, E. P.; Lutz, M.; Spek, A. L.; Hage, R.; Feringa, B. L.; Münck, E.; Que, L. J. End-on and Side-on Peroxo Derivatives of Non-Heme Iron Complexes with Pentadentate Ligands: Models for Putative Intermediates in Biological Iron/Dioxygen Chemistry. *Inorg. Chem.* **2003**, *42*, 2639−2653.
(35) Ho, R. Y. N.; Roelfes, G.; Feringa, B. L.; Que, L. Raman Evidence for a Weakened O - O Bond in Mononuclear Low-Spin Iron (III) - Hydroperoxides Iron - Peroxo Species Have Been Proposed or Demonstrated To. *J. Am. Chem. Soc.* **1999**, *121*, 264−265.
(36) Kamachi, T.; Lee, Y.-M.; Nishimi, T.; Cho, J.; Yoshizawa, K.; Nam, W. Combined Experimental and Theoretical Approach To Understand the Reactivity of a Mononuclear Cu(II)â'Hydroperoxo Complex in Oxygenation Reactions. *J. Phys. Chem. A* **2008**, *112*, 13102−13108.
(37) Hicks, S. D.; Kim, D.; Xiong, S.; Medvedev, G. A.; Caruthers, J.; Hong, S.; Nam, W.; Abu-Omar, M. Non-Heme Manganese Catalysts for On-Demand Production of Chlorine Dioxide in Water and Under Mild Conditions. *J. Am. Chem. Soc.* **2014**, *136*, 3680−3686.
(38) Leto, D. F.; Ingram, R.; Day, V. W.; Jackson, T. A. Spectroscopic Properties and Reactivity of a Mononuclear Oxomanganese(IV) Complex. *Chem. Commun.* **2013**, *49*, 5378−5380.
(39) Cho, K.; Shaik, S.; Nam, W. Theoretical Investigations into C − H Bond Activation Reaction by Nonheme Mn. *J. Phys. Chem. Lett.* **2012**, *3*, 2851−2856.
(40) Li, Q.; van der Wijst, M. G. P.; Kazemier, H. G.; Rots, M. G.; Roelfes, G. Efficient Nuclear DNA Cleavage in Human Cancer Cells by Synthetic Bleomycin Mimics. *ACS Chem. Biol.* **2014**, *9*, 1044−1051.
(41) Jackson, C. S.; Kodanko, J. J. Iron-Binding and Mobilization from Ferritin by Polypyridyl Ligands. *Metallomics* **2010**, *2*, 407−411.
(42) Zuo, J.; Schmitt, S. M.; Zhang, Z.; Prakash, J.; Fan, Y.; Bi, C.; Kodanko, J. J.; Dou, Q. P. Novel Polypyridyl Chelators Deplete Cellular Zinc and Destabilize the X-Linked Inhibitor of Apoptosis Protein (XIAP) Prior to Induction of Apoptosis in Human Prostate and Breast Cancer Cells. *J. Cell. Biochem.* **2012**, *113*, 2567−2575.
(43) Levina, A.; Crans, D. C.; Lay, P. A. Speciation of Metal Drugs, Supplements and Toxins in Media and Bodily Fluids Controls in Vitro Activities. *Coord. Chem. Rev.* **2017**, *352*, 473−498.
(44) Haas, K. L.; Franz, K. J. Application of Metal Coordination Chemistry To Explore and Manipulate Cell Biology. *Chem. Rev.* **2009**, *109*, 4921−4960.
(45) Stoving Dam, C.; Alejo Perez Henarejos, S.; Tsolakou, T.; Alexander Segato, C.; Gammelgaard, B.; Yellol, G. S.; Ruiz, J.; Henry Lambert, I.; Sturup, S. In Vitro Characterization of a Novel C{,}N-Cyclometalated Benzimidazole Ru(Ii) Arene Complex: Stability{,} Intracellular Distribution and Binding{,} Effects on Organic Osmolyte Homeostasis and Induction of Apoptosis. *Metallomics* **2015**, *7*, 885−895.
(46) Casini, A. Exploring the Mechanisms of Metal-based Pharmacological Agents via an Integrated Approach. *J. Inorg. Biochem.* **2012**, *109*, 97−106.
(47) Clède, S.; Policar, C. Metal−Carbonyl Units for Vibrational and Luminescence Imaging: Towards Multimodality. *Chem. - Eur. J.* **2015**, *21*, 942−958.
(48) Pechlaner, M.; Sigel, R. K. O. In *Characterization of Metal Ion-Nucleic Acid Interactions in Solution BT - Interplay between Metal Ions and Nucleic Acids*; Sigel, A., Sigel, H., Sigel, R. K. O., Eds.; Springer: Dordrecht, The Netherlands, 2012; pp 1−42.
(49) Sigel, A.; Sigel, H.; Freisinger, E.; Sigel, R. K. O. *Metallo-Drugs: Development and Action of Anticancer Agents*; De Gruyter: Berlin, 2018.
(50) Puckett, C. A.; Ernst, R. J.; Barton, J. K. Exploring the Cellular Accumulation of Metal Complexes. *Dalton Trans.* **2010**, *39*, 1159−1170.
(51) la Crois, R. Manganese Complexes as Catalysts in Epoxidation Reactions: A Ligand Approach. Dissertation, University of Groningen, Groningen, The Netherlands, 2000.
(52) Smith, J. R. L.; Masheder, D. Amine Oxidation. Part IX. The Electrochemical Oxidation of Some Tertiary Amines: The Effect of Structure on Reactivity. *J. Chem. Soc., Perkin Trans. 2* **1976**, *53*, 47−51.
(53) Zweig, A.; Hodgson, W. G.; Jura, W. H. The Oxidation of Methoxybenzenes. *J. Am. Chem. Soc.* **1964**, *86*, 4124−4129.
(54) Jackson, C. S.; Kodanko, J. J. Iron-Binding and Mobilization from Ferritin by Polypyridyl Ligands. *Metallomics* **2010**, *2*, 407−411.
(55) Irving, H.; Williams, R. J. P. The Stability of Transition-Metal Complexes. *J. Chem. Soc.* **1953**, *637*, 3192−3210.

DOI: 10.1021/acs.inorgchem.8b00714
Inorg. Chem. 2018, 57, 7748−7756

(56) Slater, T. F.; Sawyer, B.; Sträuli, U. Studies on Succinate-Tetrazolium Reductase Systems. *Biochim. Biophys. Acta* **1963**, *77*, 383−393.
(57) Cory, A. H.; Owen, T. C.; Barltrop, J. A.; Cory, J. G. Use of an Aqueous Soluble Tetrazolium/Formazan Assay for Cell Growth Assays in Culture. *Cancer Commun.* **1991**, *3*, 207−212.
(58) Wang, H. Z.; Chang, C. H.; Lin, C. P.; Tsai, M. C. Using MTT Viability Assay to Test the Cytotoxicity of Antibiotics and Steroid to Cultured Porcine Corneal Endothelial Cells. *J. Ocul. Pharmacol. Ther.* **1996**, *12*, 35−43.
(59) Ulukaya, E.; Colakogullari, M.; Wood, E. J. Interference by Anti-Cancer Chemotherapeutic Agents in the MTT-Tumor Chemosensitivity Assay. *Chemotherapy* **2004**, *50*, 43−50.
(60) Wang, Y. J.; Zhou, S. M.; Xu, G.; Gao, Y. Q. Interference of Phenylethanoid Glycosides from Cistanche Tubulosa with the MTT Assay. *Molecules* **2015**, *20*, 8060−8071.
(61) van Tonder, A.; Joubert, A. M.; Cromarty, A. D. Limitations of the 3-(4,5-Dimethylthiazol-2-Yl)-2,5-Diphenyl-2H-Tetrazolium Bromide (MTT) Assay When Compared to Three Commonly Used Cell Enumeration Assays. *BMC Res. Notes* **2015**, *8*, 47−48.
(62) Holder, A. L.; Goth-Goldstein, R.; Lucas, D.; Koshland, C. P. Particle-Induced Artifacts in the MTT and LDH Viability Assays. *Chem. Res. Toxicol.* **2012**, *25*, 1885−1892.
(63) Pozzolini, M.; Scarfi, S.; Benatti, U.; Giovine, M. Interference in MTT Cell Viability Assay in Activated Macrophage Cell Line. *Anal. Biochem.* **2003**, *313*, 338−341.
(64) Vellonen, K. S.; Honkakoski, P.; Urtti, A. Substrates and Inhibitors of Efflux Proteins Interfere with the MTT Assay in Cells and May Lead to Underestimation of Drug Toxicity. *Eur. J. Pharm. Sci.* **2004**, *23*, 181−188.
(65) Setsukinai, K.; Urano, Y.; Kakinuma, K.; Majima, H. J.; Nagano, T. Development of Novel Fluorescence Probes That Can Reliably Detect Reactive Oxygen Species and Distinguish Specific Species. *J. Biol. Chem.* **2003**, *278*, 3170−3175.
(66) Morley, N.; Curnow, A.; Salter, L.; Campbell, S.; Gould, D. N-Acetyl-L-Cysteine Prevents DNA Damage Induced by UVA, UVB and Visible Radiation in Human Fibroblasts. *J. Photochem. Photobiol., B* **2003**, *72*, 55−60.
(67) Sun, S. Y. N-Acetylcysteine, Reactive Oxygen Species and Beyond. *Cancer Biol. Ther.* **2010**, *9*, 109−110.
(68) Zafarullah, M.; Li, W. Q.; Sylvester, J.; Ahmad, M. Molecular Mechanisms of N-Acetylcysteine Actions. *Cell. Mol. Life Sci.* **2003**, *60*, 6−20.
(69) Speisky, H.; Gómez, M.; Burgos-Bravo, F.; López-Alarcón, C.; Jullian, C.; Olea-Azar, C.; Aliaga, M. E. Generation of Superoxide Radicals by Copper-Glutathione Complexes: Redox-Consequences Associated with Their Interaction with Reduced Glutathione. *Bioorg. Med. Chem.* **2009**, *17*, 1803−1810.
(70) Takamizawa, S.; Maehata, Y.; Imai, K.; Senoo, H.; Sato, S.; Hata, R.-I. Effects of Ascorbic Acid and Ascorbic Acid 2-Phosphate, a Long-Acting Vitamin C Derivative, on the Proliferation and Differentiation of Human Osteoblast-like Cells. *Cell Biol. Int.* **2004**, *28*, 255−265.
(71) Hata, R.-I.; Senoo, H. L-Ascorbic Acid 2-Phosphate Stimulates Collagen Accumulation, Cell Proliferation, and Formation of a Three-Dimensional Tissuelike Substance by Skin Fibroblasts. *J. Cell. Physiol.* **1989**, *138*, 8−16.
(72) Olive, P. L. Detection of DNA Damage in Individual Cells by Analysis of Histone H2AX Phosphorylation. *Methods Cell Biol.* **2004**, *75*, 355−373.
(73) Rogakou, E. P.; Boon, C.; Redon, C.; Bonner, W. M. Megabase Chromatin Domains Involved in DNA Double-Strand Breaks in Vivo. *J. Cell Biol.* **1999**, *146*, 905−916.
(74) Takahashi, A.; Ohnishi, T. Does GammaH2AX Foci Formation Depend on the Presence of DNA Double Strand Breaks? *Cancer Lett.* **2005**, *229*, 171−179.
(75) Bonner, W. M.; Redon, C. E.; Dickey, J. S.; Nakamura, A. J.; Sedelnikova, O. A.; Solier, S.; Pommier, Y. GammaH2AX and Cancer. *Nat. Rev. Cancer* **2008**, *8*, 957−967.
(76) Davies, C. W.; Chaney, J.; Korbel, G.; Ringe, D.; Petsko, G. A.; Ploegh, H.; Das, C. The Co-Crystal Structure of Ubiquitin Carboxy-Terminal Hydrolase L1 (UCHL1) with a Tripeptide Fluoromethyl Ketone (Z-VAE(OMe)-FMK. *Bioorg. Med. Chem. Lett.* **2012**, *22*, 3900−3904.
(77) Wu, X.; Seo, M. S.; Davis, K. M.; Lee, Y.-M.; Chen, J.; Cho, K.-B.; Pushkar, Y. N.; Nam, W. A Highly Reactive Mononuclear Non-Heme Manganese(IV)â€“Oxo Complex That Can Activate the Strong Câ€“H Bonds of Alkanes. *J. Am. Chem. Soc.* **2011**, *133*, 20088−20091.
(78) Jacob, C.; Doering, M.; Burkholz, T. The Chemical Basis of Biological Redox Control. *Redox Signaling and Regulation in Biology and Medicine*; Wiley-VCH Verlag: Weinheim, Germany, pp 63−122.
(79) Hamed, M. Y.; Silver, J.; Wilsonx, M. T. Studies of the Reactions of Ferric Iron with Glutathione and Some Related Thiols. *Inorg. Chim. Acta* **1983**, *78*, 1−11.
(80) Hamed, M. Y.; Hider, R. C.; Silver, J. The Competition between Enterobactin and Glutathione for Iron. *Inorg. Chim. Acta* **1982**, *66*, 13−18.
(81) Wang, H.; Wang, B.; Wang, M.; Zheng, L.; Chen, H.; Chai, Z.; Zhao, Y.; Feng, W. Time-Resolved ICP-MS Analysis of Mineral Element Contents and Distribution Patterns in Single Cells. *Analyst* **2015**, *140*, 523−531.
(82) Parr, R. M.; Taylor, D. M. The Concentrations of Cobalt, Copper, Iron and Zinc in Some Normal Human Tissues as Determined by Neutron-Activation Analysis. *Biochem. J.* **1964**, *91*, 424−431.
(83) Speisky, H.; Gomez, M.; Carrasco-Pozo, C.; Pastene, E.; Lopez-Alarcon, C.; Olea-Azar, C. Cu(I)-Glutathione Complex: A Potential Source of Superoxide Radicals Generation. *Bioorg. Med. Chem.* **2008**, *16*, 6568−6574.
(84) Ueda, J.; Takai, M.; Shimazu, Y.; Ozawa, T. Reactive Oxygen Species Generated from the Reaction of Copper(II) Complexes with Biological Reductants Cause DNA Strand Scission. *Arch. Biochem. Biophys.* **1998**, *357*, 231−239.
(85) Kachur, A. V.; Koch, C. J.; Biaglow, J. E. Mechanism of Copper-Catalyzed Oxidation of Glutathione. *Free Radical Res.* **1998**, *28*, 259−269.
(86) Oppenheimer, N. J.; Chang, C.; Rodriguez, L. O.; Hecht, S. M. Copper(I) . Bleomycin. A Structurally Unique Oxidation-Reduction Active Complex. *J. Biol. Chem.* **1981**, *256*, 1514−1517.
(87) Petering, D. H.; Byrnes, R. W.; Antholine, W. E. The Role of Redox-Active Metals in the Mechanism of Action of Bleomycin. *Chem.-Biol. Interact.* **1990**, *73*, 133−182.
(88) Ehrenfeld, G. M.; Shipley, J. B.; Heimbrook, D. C.; Sugiyama, H.; Long, E. C.; Van Boom, J. H.; van der Marel, G. A.; Oppenheimer, N. J.; Hecht, S. M. Copper-Dependent Cleavage of DNA by Bleomycin. *Biochemistry* **1987**, *26*, 931−942.
(89) Ehrenfeld, G. M.; Rodriguez, L. O.; Hecht, S. M.; Chang, C.; Basus, V. J.; Oppenheimer, N. J. Copper(I)-Bleomycin: Structurally Unique Complex That Mediates Oxidative DNA Strand Scission. *Biochemistry* **1985**, *24*, 81−92.
(90) Ponka, P.; Beaumont, C.; Richardson, D. R. Function and Regulation of Transferrin and Ferritin. *Semin. Hematol.* **1998**, *35*, 35−54.

DOI: 10.1021/acs.inorgchem.8b00714
Inorg. Chem. 2018, 57, 7748−7756